

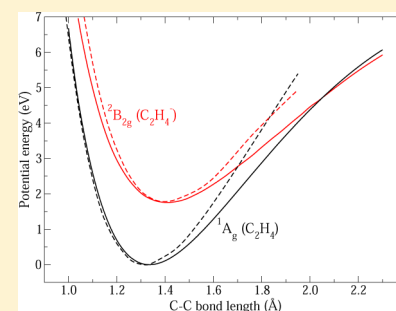
Determination of the Resonance Energy and Width of the ${}^2B_{2g}$ Shape Resonance of Ethylene with the Method of Analytical Continuation in the Coupling Constant

Jiří Horáček,[†] Ivana Paidarová,[‡] and Roman Čurík*[‡]

[†]Institute of Theoretical Physics, Faculty of Mathematics and Physics, Charles University, V Holešovičkách 2, 180 00 Praha 8, Czech Republic

[‡]J. Heyrovský Institute of Physical Chemistry, Academy of Sciences of the Czech Republic, v.v.i., Dolejškova 3, 182 23 Prague 8, Czech Republic

ABSTRACT: The method of analytical continuation in the coupling constant, which allows us to determine the energy and width of a shape resonance, has been applied to the study of the ${}^2B_{2g}$ shape resonance of ethylene. The procedure was done in two steps. In the first step, we used commercially available quantum-chemistry programs to calculate the electronic energy of a neutral molecule and of a negative ion. In both calculations, the Hamiltonian was altered by the inclusion of an additional attractive potential that helps to keep the negative ion bound. In the second step, the energy difference between the neutral molecule and its negative ion was analytically continued by the use of the statistical Padé approximation.



INTRODUCTION

Ethylene, C_2H_4 , belongs to a class of simple hydrocarbon molecules that are present in the edge plasma of fusion reactors. They result from erosion of the reactor walls due to plasma-wall interactions.¹ Collisional processes of electrons with these hydrocarbon species may play a role determining the stability and equilibrium conditions of the plasma bulk. Ethylene is also present in planetary atmospheres.² It has been identified as a source of significant infrared absorption in the atmospheres of Jupiter, Saturn, and Titan,³ while in the Earth's atmosphere it plays the role of a pollutant. It is produced by various sources such as road traffic and biomass burning, and it has wide applications in agriculture, where for example it serves as a natural plant hormone used to force the ripening of fruits.⁴

As a result of the interest from these various fields, a considerable amount of experimental and theoretical work has been devoted to the study of low-energy collisions of electrons with ethylene. A dominant feature appearing in the elastic and vibrationally inelastic scattering at low energies is the ${}^2B_{2g}$ π^* shape resonance, which was first seen in transmission experiments.⁵ It has been demonstrated experimentally that this resonance drives vibrational excitation of several symmetric modes at low energies⁶ with a hint of weak boomerang structure centered around a collision energy of 1.8 eV. The boomerang structure of the inelastic cross section was later unambiguously confirmed in excitation of higher overtones of the C–C symmetric stretch mode.⁷ Several measurements^{8,9} have shown that the resonance is strong and visible also in the elastic channel. It is important to note that very recent dissociative electron attachment (DEA) experiments¹⁰ did not observe any anion fragments for collision energies under 6 eV.

The ${}^2B_{2g}$ π^* resonance lies well below the DEA thresholds, and thus, the resonance does not appear to play any role in the DEA processes of ethylene.

The ${}^2B_{2g}$ resonance has also been the subject of several theoretical studies. Donnelly¹¹ attempted to stabilize the resonance by application of a complex scaling method combined with a second-order propagator. However, the resulting resonance width appeared to be very unstable with respect to the choice of Gaussian basis set. Another attempt with a one-electron propagator method resulted in the correct vertical energy, but the predicted width of the resonance was too narrow.¹² Schneider et al.¹³ employed complex Kohn variational calculations and clearly showed that the ${}^2B_{2g}$ partial cross section is dominated by a resonance at 1.84 eV with a width of 0.46 eV. These results appear to be the first theoretical calculations that agree quantitatively with the experimental evidence described above. The complex Kohn scattering calculations were later refined,¹⁴ and the full resonant curve of the transient negative ion $C_2H_4^-$ was obtained. The latter authors used the Hartree–Fock approximation to describe the target C_2H_4 state and only singly excited configurations of the target were used after addition of the continuum electron. More recently, the Schwinger multichannel method was applied to compute the elastic cross section for ethylene.¹⁵ While the ${}^2B_{2g}$ resonance is very clearly positioned in their cross sections at 2.0 eV, the authors did not mention the corresponding resonance

Special Issue: Franco Gianturco Festschrift

Received: March 28, 2014

Revised: June 20, 2014

Published: June 23, 2014

width. The resonance position of 1.98 eV was also reported very recently¹⁶ as a result of UK molecular R-matrix calculations.

Therefore, one of goals of the present study was to determine the resonance position and width as a function of the C–C bond distance of ethylene by the use of a higher-order correlation method than in previous scattering studies.^{13,14} Namely, we employed the coupled-cluster level of theory. Moreover, the present calculations employed the analytical continuation in the coupling constant (ACCC) method^{17,18} extended by the use of the statistical Padé approximation.¹⁹ The ab initio data that form an input to the ACCC method are vertical attachment energies. In order to stabilize the energy of the resonant state, we used the method of Nestmann and Peyerimhoff,^{20,21} in which the molecular Hamiltonian is altered by the addition of a one-electron attractive force that binds the resonance. In the present study, this attractive force was represented by positive charges λ added to all of the nuclei. The idea was to use standard quantum-chemistry codes designed to calculate bound-state energies of the target molecule and its anion with variable nuclear charges. The resulting curve of the vertical attachment energy as a function of coupling constant λ was then processed by the ACCC method described in the following section. Since the necessary quantum-chemistry computations involved only bound states of the neutral molecule and its negative ion, we could apply the CCSD-T level of theory. Although CCSD-T represents a gold standard of quantum chemistry, its implementation in scattering theory appears to be very difficult. In the present study, we did not attempt to solve this problem; we merely present a method that is able to determine some of the scattering results (resonance parameters) at the CCSD-T level of theory.

■ ANALYTICAL CONTINUATION IN THE COUPLING CONSTANT

To calculate bound-state energies and their square-integrable wave functions is now a routine task even for large polyatomic molecules, and many commercial programs are available. However, the calculation of resonance energies and their widths is a serious problem. It is therefore natural to ask whether one can obtain the resonance energy and perhaps even its width from a knowledge of the bound-state energies alone. This problem has been studied, and some approximate results were obtained (see, e.g., ref 20). Here we describe one method developed in the field of nuclear physics that in principle is able to provide the resonance energy and also the resonance width to a high degree of accuracy using only bound-state energies as input, the so-called method of analytical continuation in the coupling constant. The ACCC method works as follows.²² Let us for simplicity assume that motion of the electron in the vicinity of a molecule is determined by a Hamiltonian H that generates a resonance at an energy E given by

$$E = E_R - \frac{i}{2}\Gamma \quad (1)$$

where E_R is the resonance energy and Γ is the resonance width. Let us now add to the original potential H an attractive short-range interaction U multiplied by a real positive parameter λ :

$$H \rightarrow H + \lambda U \quad (2)$$

As λ increases, the new Hamiltonian H becomes more attractive, and some resonance states are eventually transformed into bound states. It has been shown²² that a naive

extrapolation of the energy in terms of λ , $E \approx E_0 + E_1\lambda + E_2\lambda^2 + \dots$, as is sometimes used in quantum chemistry, is not sufficient to get both the resonance energy and the resonance width and that the extrapolations must be replaced by an analytical continuation. In addition, the parameter used for the continuation is not the parameter λ itself but a new variable $y = (\lambda - \lambda_0)^{1/2}$, which will be discussed below. The function to be analytically continued is the momentum $k(\lambda(y))$, where $k^2/2 = E$. The ACCC method was introduced by Krasnopolsky and Kukulin^{17,18} and is described in detail in a monograph.²² The ACCC approach has found several applications, mainly in nuclear physics (see, e.g., refs 23–27). Recently, Horáček et al.¹⁹ and Papp et al.²⁸ applied the ACCC method to real molecular resonances, discussing the $^2\Pi_g^-$ state of the N_2^- resonance of molecular nitrogen and resonances of amino acid molecules (alanine, glycine, and valine), proving that the ACCC method can yield accurate resonance energies and widths for nonmodel situations based on data obtained using standard quantum-chemistry codes.

In this work, we carried out the analytic continuation by using the so-called statistical Padé approximation (Padé III approximation).²² This approach has several advantages: (1) it allows us to use low-order Padé approximations even if a large number of points are available; (2) it allows us to take into account the inaccuracy of the input data; (3) it can describe a much broader range of functions, such as functions with poles and cuts; (4) it carries out the analytical continuation automatically; and so on. Since an absolute majority of molecular resonances possess nonzero angular momentum l , we will consider here the ACCC method for $l \neq 0$. The situation for $l = 0$ is more complicated and will not be discussed here. As has already been shown (see, e.g., ref 22), at small values of k the function $k(\lambda)$ behaves as $k(\lambda) \approx a(\lambda - \lambda_0)^{1/2}$, where λ_0 denotes the point $k(\lambda_0) = 0$. At smaller values of λ (i.e., $\lambda < \lambda_0$), $k(\lambda)$ becomes complex, and the resonance energy acquires its imaginary part.

The standard ACCC method is in fact a two-step method requiring two fits. In the first step the bifurcation point λ_0 is determined, and then by the second fit the resonance energy and width are computed. We observed that the final values of the resonance parameters are very sensitive to the precise value of the bifurcation point λ_0 . Even minor changes in the λ_0 value may lead to significant changes of the obtained resonance parameters. There is, however, another much simpler modification of the ACCC method that requires only one function to be fitted. This approach is based on the analytical continuation of the function $\lambda(\kappa)$ [the inverse function to the function $\kappa(\lambda)$], where $k = i\kappa$. For this reason, we will call this modification the inverse ACCC (IACCC) method. Let us start from the first fit of the ACCC method:

$$\lambda(\kappa) \approx \frac{P_N(\kappa)}{Q_M(\kappa)} \quad (3)$$

Then the resonance parameters may be obtained by solving the simple polynomial equation

$$P_N(k) = 0. \quad (4)$$

The process of determining the bifurcation point λ_0 is implicitly involved in this procedure and need not be carried out separately. In addition, this approach may in principle be able to determine the positions of virtual states and of other resonances because solving eq 4 provides us with N solutions.

The standard ACCC method allows for the determination of only one resonance that is connected with the bound-state region through the origin. At first sight this method looks extremely simple, even trivial, but obtaining stable accurate results in real applications is a rather complicated task.

Let us first of all mention the calculation of the Padé approximation. In the present application, we used the so-called statistical Padé approximation (Padé III approximation). The type-III Padé approximant of order $[N, M]$ representing a set of empirical values f_i ($i = 1, 2, \dots, J$) of a function $f(x)$ measured at points x_i with statistical errors ε_i is defined as the rational function $P_N(x)/Q_M(x)$, where

$$P_N(x) = \sum_{i=0}^N p_i x^i, \quad Q_M(x) = 1 + \sum_{k=1}^M q_k x^k \quad (5)$$

are polynomials of degrees N and M , respectively (with $M + N < J - 1$) that minimize the functional

$$\chi^2 = \sum_{i=1}^J \frac{1}{\varepsilon_i^2} \left[\frac{P_N(x_i)}{Q_M(x_i)} - f_i \right]^2 \quad (6)$$

Since in the present case no information on the errors is available, we kept all of the weights constant (i.e., $\varepsilon_i = 1.0$). The minimization of χ^2 represents a nonlinear problem with a complicated surface that may possess many local minima, some of which may have very small values of χ^2 but give very different values of resonance energies and widths (for more details, see, e.g., refs 29–33).

The second problem is the right choice of the parameters N and M . If the values of N and M are too small, the approximation cannot describe correctly all of the physics, and the obtained values of the resonance energies and widths may be very imprecise. As N and M are increased, however, a serious difficulty arises, namely, the appearance of so-called Froissard doublets.³⁴ A Froissard doublet is a pair consisting of a pole and a zero of the Padé approximation between which the distance is very small. In this case, the polynomials $P_N(x)$ and $Q_M(x)$ have almost identical roots. These doublets cluster around a circle with the center at the origin. The appearance of Froissard doublets is characteristic of the Padé approximation and seriously limits its application. If such a doublet appears close to the true position of the resonance, the accurate determination of the resonance energy and width is almost impossible.

The third problem is the selection of the data to be used for the continuation process. One would expect that the data at the lowest energies, which are as close to the resonance as possible, would be the best choice. This might be true in the case of very accurate data. In reality, however, the accuracy of the calculated bound-state energies is rather limited, and one could expect that the relative accuracy decreases as the bound-state energy approaches the threshold simply because no finite set of compact functions (typically represented by Gaussian functions) can accurately describe spatially very extended wave functions.

Other open questions include how many points to use in the calculation the Padé approximation and the energy at which to stop, but probably the most important question is how to choose the perturbation potential U . For simplicity, in this present application we used the potential U in the form of Coulomb potential. This is not the best choice from the point of accuracy, but it greatly simplifies the use of quantum-

chemistry codes. Moreover, to get stable and accurate results, one must also consider the analytical structure of the function to be represented by the Padé approximation. As mentioned above, at small values of k the function $k(\lambda)$ behaves as $k(\lambda) \approx a(\lambda - \lambda_0)^{1/2}$, where λ_0 denotes the point $k(\lambda_0) = 0$. Hence, the function $\lambda(\kappa)$ must have its minimum at the origin

$$\lambda(\kappa) \approx \lambda_0 + \lambda_2 \kappa^2 + \lambda_3 \kappa^3 + \dots \quad (7)$$

In order to comply with the low-energy behavior of the function $\lambda(\kappa)$ in eq 7, in the present calculations we represented it as

$$\lambda(\kappa) \approx \frac{\lambda_0 + \lambda_2 \kappa^2 + \lambda_3 \kappa^3 + \dots}{1 + \mu_2 \kappa^2 + \mu_3 \kappa^3 + \dots} = \frac{P_N(\kappa)}{Q_M(\kappa)} \quad (8)$$

In the case of very precise data for a d wave (as in the present study of the ${}^2B_{2g}$ resonance), we could also omit the κ^3 terms. However, for real quantum-chemistry computations this does not improve the accuracy and stability of the calculation because the representation of $\lambda(\kappa)$ in the form of the Padé approximation (eq 8) is approximative anyway [e.g., it ignores possible square-root-type singularities of $\lambda(\kappa)$]. The calculation now proceeds as follows: for a given N and M and the minimal and maximal energies E_{\min} and E_{\max} the polynomials P_N and Q_M are obtained and their roots calculated. If the value of χ^2 is sufficiently small and the calculated resonance position is found to be far enough from the roots of Q_M , the result is considered to be acceptable. Then the calculation is repeated for other parameters to obtain a range of resonance positions. For good data the spread in the resonance parameters is on the order of ± 20 meV on average.

■ QUANTUM-CHEMISTRY COMPUTATIONS

Ab initio calculations were done using the CCSD-T method^{35,36} as implemented in the MOLPRO 10 package of quantum-chemistry programs³⁷ and Dunning's augmented correlation-consistent basis set of quadruple- ζ quality (aug-cc-pVQZ).³⁸ The equilibrium configuration given by the CCSD-T method and the aug-cc-pVQZ basis set is defined by the following parameters: the bond distances $R_{C-C} = 1.339$ Å and $R_{H-C} = 1.086$ Å and the C–C–H angle of 121.2° .

The function $\lambda(\kappa)$ in eqs 3 and 8 is determined from the inverse function $\Delta E(\lambda) = \kappa^2(\lambda)/2$. The symbol $\Delta E(\lambda)$ stands for the vertical electron affinity:

$$\Delta E(\lambda) = E^0(\lambda) - E^-(\lambda) \quad (9)$$

in which the energy $E^0(\lambda)$ represents the ground-state energy of the ethylene molecule and the energy $E^-(\lambda)$ is the ground-state energy of ethylene anion. Both energies were obtained under the influence of an additional Coulomb field created by additional charges λ positioned at all of the nuclear centers. The parameter λ was varied from 0.001 to 0.1 au in steps of 0.001 au. Depending on R_{C-C} , this required 40 to 90 points to describe the $\Delta E(\lambda)$ curve. The internuclear distance R_{C-C} was also varied from 1.04 to 2.4 Å. Typical behavior of the vertical electron affinity $\Delta E(\lambda)$ for three selected values of R_{C-C} is shown in Figure 1. It can be seen that the ethylene molecule requires a weaker additional Coulomb field to stabilize and bind the ${}^2B_{2g}$ shape resonance at larger R_{C-C} . Furthermore, we excluded data with binding energies under 1 eV in order to avoid basis set effects in the long-range Coulomb field. A more detailed discussion of this topic with a numerical analysis can be found in ref 19.

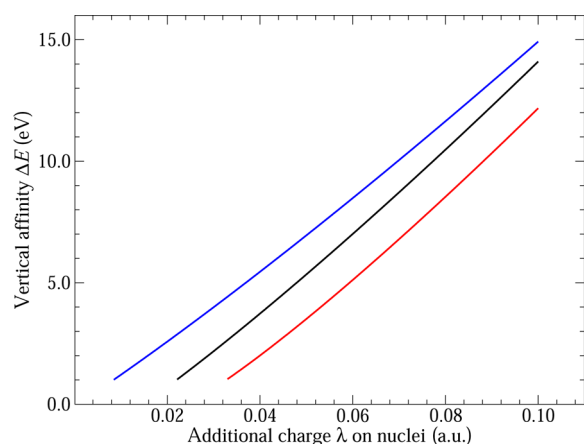


Figure 1. Vertical electron affinity $\Delta E(\lambda)$ as a function of the parameter λ for three internuclear distances $R_{C-C} = 1.04$ Å (red curve), 1.34 Å (black curve), and 2.0 Å (blue curve).

RESULTS AND DISCUSSION

The calculated resonance positions and widths for different separations R_{C-C} are summarized in Table 1. The remaining geometric parameters (R_{H-C} and the C–C–H angle) were kept fixed at the equilibrium values listed in the previous section. For each reported value, the number after the \pm symbol indicates the spread of the value obtained by modifying a set of

Table 1. Resonance Energies and Widths of the ${}^2B_{2g}$ State of Ethylene Calculated at a Set of Internuclear Distances R_{C-C} ^a

R_{C-C} (Å)	energy (eV)	width (eV)
1.04	2.307 ± 0.084	1.715 ± 0.154
1.08	2.375 ± 0.054	1.524 ± 0.131
1.12	2.385 ± 0.054	1.274 ± 0.120
1.16	2.329 ± 0.048	1.102 ± 0.125
1.20	2.264 ± 0.037	0.937 ± 0.103
1.24	2.176 ± 0.026	0.766 ± 0.066
1.28	2.055 ± 0.016	0.635 ± 0.053
1.32	1.918 ± 0.011	0.511 ± 0.034
1.34	1.856 ± 0.007	0.467 ± 0.021
1.36	1.788 ± 0.005	0.417 ± 0.016
1.40	1.649 ± 0.004	0.334 ± 0.009
1.44	1.508 ± 0.003	0.268 ± 0.008
1.48	1.365 ± 0.005	0.218 ± 0.014
1.52	1.240 ± 0.005	0.147 ± 0.018
1.56	1.109 ± 0.004	0.115 ± 0.016
1.60	0.984 ± 0.006	0.090 ± 0.014
1.64	0.859 ± 0.007	0.073 ± 0.011
1.70	0.694 ± 0.008	0.045 ± 0.010
1.76	0.522 ± 0.012	0.043 ± 0.005
1.80	0.439 ± 0.006	0.024 ± 0.005
1.84	0.350 ± 0.014	0.021 ± 0.005
1.88	0.258 ± 0.010	0.016 ± 0.002
1.92	0.192 ± 0.009	0.009 ± 0.001
1.96	0.124 ± 0.008	0.005 ± 0.001
2.00	0.084 ± 0.007	0.002 ± 0.001
2.04	0.012 ± 0.009	0.000 ± 0.001
2.20	−0.111 ± 0.004	0.000 ± 0.001
2.30	−0.145 ± 0.013	0.000 ± 0.001

^aThe numbers following the \pm symbols serve as estimations of the accuracy of the respective values. For a more detailed explanation, see the text.

parameters used in the determination of the Padé approximation (eq 3). In particular, the following parameters were varied: the polynomial orders N and M , the number of points selected from the $\Delta E(\lambda)$ curves (displayed in Figure 1), and the lowest and highest energies of the $\Delta E(\lambda)$ curve chosen for the process of analytical continuation. These quantities serve as estimations of the stability of the procedure of analytical continuation with respect to the parameters that cannot be determined beforehand and must be found during the data analysis. We believe that these numbers represent the accuracy of the described continuation process. However, these errors represent only estimates of the stability of the analytical continuation method. The errors arising from the quality of CCSD-T theory, incompleteness of basis set, or systematic errors are difficult to estimate and are not included.

The calculated energies and widths of the ${}^2B_{2g}$ shape resonance are displayed in Figure 2. We compare our results

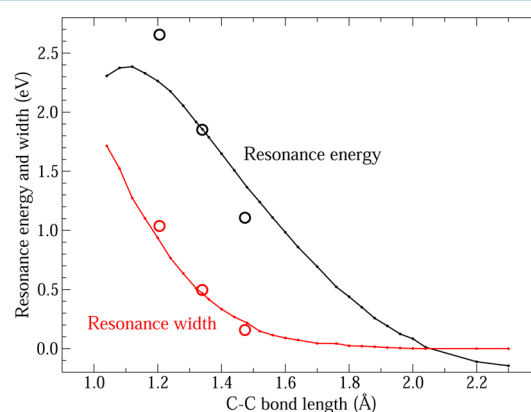


Figure 2. Resonance position and width as functions of the bond length R_{C-C} . Circles denote the results of previous complex Kohn scattering calculations.¹⁴

with three data points obtained previously by scattering calculations employing the complex Kohn method.¹⁴ In the latter work, the authors used the Hartree–Fock method to describe the neutral target C_2H_4 . In the description of the resonant ${}^2B_{2g}$ state, the authors applied the so-called Relaxed-SCF approximation, in which the target’s relaxation in the presence of the scattered electron is formed by singly excited determinants that belong to the same symmetry as the reference Slater determinant describing the neutral target molecule. Figure 2 demonstrates that this approximate modeling of the target’s response to the presence of the scattered electron in the ${}^2B_{2g}$ resonant state results in resonance widths that are in a very good accord with the present results based on coupled-cluster (CCSD-T) theory. The agreement is less satisfactory in the case of the resonance energy. At the equilibrium geometry $R_{C-C} = 1.339$ Å, we again get excellent agreement with the previous calculations: the present results give $E_R = 1.856$ eV, while the complex Kohn computations yielded $E_R = 1.852$ eV. However, for shorter R_{C-C} we obtained lower resonance energies, while for larger R_{C-C} our values surpass those of the previous calculations.

These differences are also visible in Figure 3, which displays potential energy curves for the 1A_g ground state of the neutral target molecule and the ${}^2B_{2g}$ negative ion resonance. It can be clearly seen that the Hartree–Fock description of the neutral target state leads to higher R_{C-C} dissociation energy compared with the present CCSD-T dissociation curve. The second

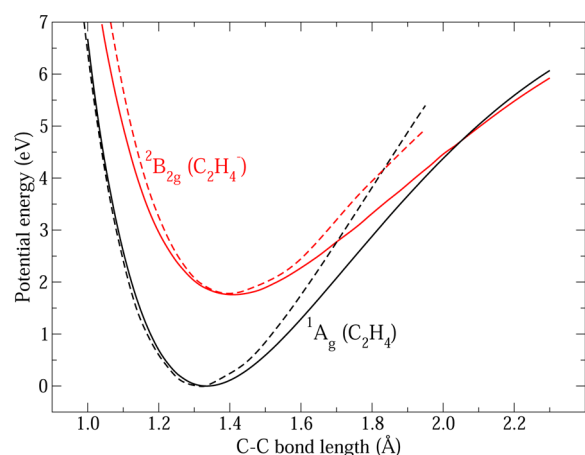


Figure 3. Potential energy curve for the 1A_g ground state of the neutral C_2H_4 molecule (solid black line) and resonant energy curve of the temporary $^2B_{2g}$ negative ion state (solid red line) as functions of C–C bond length obtained by the present approach. The results of the complex Kohn calculations¹⁴ are displayed with corresponding dashed lines.

visible difference between the two calculations is the crossing point of the neutral and anionic curves. The crossing point defines the value of R_{C-C} beyond which the resonant state becomes bound. The crossing point obtained in the present work ($R_{C-C} = 2.04 \text{ \AA}$) is further away from equilibrium compared with that found in the complex Kohn calculations ($R_{C-C} = 1.82 \text{ \AA}$). A summary of all of the theoretical results for the energy and width of the $^2B_{2g}$ resonance at the equilibrium geometry is given in Table 2.

Table 2. Comparison of Other Theoretical Results with Those of the Present Calculation at the Equilibrium Distance

energy (eV)	width (eV)	source
1.94	0.110	ref 11
2.49	0.234	ref 11
1.88	0.442	ref 11
1.86	0.18	ref 12
1.89	0.18	ref 12
1.83	0.460	ref 13
1.852	0.496	ref 14
2.0	N/A	ref 15
1.98	N/A	ref 16
1.856	0.467	present work

CONCLUSIONS

In summary, we would like to emphasize that in the present study we combined two very different techniques that allowed us to determine the $^2B_{2g}$ resonance energies and widths of ethylene. The first technique was carried as a first step in which we computed vertical affinities of ethylene submerged into an attractive Coulomb field parametrized by variable additional nuclear charges λ . This additional attractive interaction stabilized the resonance state and made it bound. The technique allowed us to employ a quantum-chemistry method with an advanced correlation treatment, namely, CCSD-T, to perform the bound-state calculations for the neutral molecule and for the negative ion.

In the second step, we applied the method of analytical continuation in the coupling constant, which enabled us to determine not only the resonance energy (often seen in the literature as the extrapolation $\lambda \rightarrow 0$) but also the resonance width. The computed resonance energy and width at the equilibrium geometry agree very well with the results of previous scattering calculations using the complex Kohn method.¹⁴ Upon variation of R_{C-C} , the agreement between the resonance widths holds but resonance energy determined by complex Kohn method follows a steeper descent compared with the present results.

The computed potential energy surfaces for the neutral C_2H_4 molecule and the transient negative ion $C_2H_4^-$ suggest that the $^2B_{2g}$ resonance does not play any role in the dissociative electron attachment process. This suggestion is in accord with the experimental evidence,¹⁰ in which the authors found no negative ion signal at collision energies under 7–8 eV. On the other hand, the shapes of the computed energy surfaces do suggest the existence of the boomerang mechanism in the process of vibrational excitation by electron impact. These boomerang oscillations in vibrationally inelastic cross sections were seen experimentally for excitation of the CH_2 bending mode (ν_3)⁶ and for excitation of the C–C symmetric stretch mode (ν_2).⁷ The obtained data may serve as an input for the construction of the boomerang model describing the vibrational excitation of ethylene by impact of low-energy electrons.

AUTHOR INFORMATION

Corresponding Author

*E-mail: roman.curik@jh-inst.cas.cz.

Notes

The authors declare no competing financial interest.

ACKNOWLEDGMENTS

This work was supported by the Grant Agency of the Czech Republic (GAČR). J.H. and I.P. acknowledge the support of Grant P203/12/0665. R.Č. acknowledges the support of Grant P208/11/0452. The authors would like to thank the anonymous reviewer for the invaluable comments and suggestions to improve the quality of the paper.

REFERENCES

- (1) Fantz, U.; Meir, S.; ASDEX Upgrade Team. Correlation of the Intensity Ratio of C_2/CH Molecular Bands with the Flux Ratio of C_2H_2/CH_4 Particles. *J. Nucl. Mater.* **2005**, *337*, 1087–1091.
- (2) Roe, H.; de Pater, I.; McKay, C. Seasonal Variation of Titan's Stratospheric Ethylene (C_2H_4) Observed. *Icarus* **2004**, *169*, 440.
- (3) Bezard, B.; Moses, J.; Lacy, J.; Greathouse, T.; Richter, M.; Grith, C. Detection of Ethylene C_2H_4 on Jupiter and Saturn in Nonauroral Regions. *Bull. Am. Astron. Soc.* **2001**, *33*, 1079–1080.
- (4) Wang, K.; Li, H.; Ecker, J. R. Ethylene Biosynthesis and Signaling Networks. *Plant Cell* **2002**, *14* (Suppl.), 131–151.
- (5) Burrow, P. D.; Jordan, K. D. On the Electron Affinities of Ethylene and 1,3-Butadiene. *Chem. Phys. Lett.* **1975**, *36*, 594–598.
- (6) Walker, I. C.; Stamatovic, A.; Wong, S. F. Vibrational Excitation of Ethylene by Electron Impact: 1–11 eV. *J. Chem. Phys.* **1978**, *69*, 5532–5537.
- (7) Allan, M.; Winstead, C.; McKoy, V. Electron Scattering in Ethene: Excitation of the \tilde{a}^3B_{1u} State, Elastic Scattering, and Vibrational Excitation. *Phys. Rev. A* **2008**, *77*, No. 042715.
- (8) Lunt, S. L.; Randell, J.; Ziesel, J. P.; Mrotzek, G.; Field, D. Low-Energy Electron Scattering from CH_4 , C_2H_4 and C_2H_6 . *J. Phys. B* **1994**, *27*, 1407–1422.

- (9) Panajotovic, R.; Kitajima, M.; Tanaka, H.; Jelisavcic, M.; Lower, J.; Buckman, S. Electron Collisions with Ethylene. *Radiat. Phys. Chem.* **2003**, *68*, 233–237.
- (10) Szymańska, E.; Mason, N. J.; Krishnakumar, E.; Matias, C.; Mauracher, A.; Scheier, P.; Denifl, S. Dissociative Electron Attachment and Dipolar Dissociation in Ethylene. *Int. J. Mass. Spectrom.* **2014**, *365*, 356–364.
- (11) Donnelly, R. A. Complex Coordinate Calculation on an Ethylene Shape Resonance. *J. Chem. Phys.* **1986**, *84*, 6200–6203.
- (12) Medikeri, M. N.; Mishra, M. K. Characterization of Molecular Shape Resonances Using Different Decouplings of the Dilated Electron Propagator with Application to $^{11}\text{CO}^-$ and $^{2}\text{B}_{2g} \text{C}_2\text{H}_4^-$ Shape Resonances. *J. Chem. Phys.* **1995**, *103*, 676–682.
- (13) Schneider, B. I.; Rescigno, T. N.; Lengsfeld, B. H., III; McCurdy, C. W. Accurate Ab Initio Treatment of Low-Energy Electron Collisions with Ethylene. *Phys. Rev. Lett.* **1991**, *66*, 2728–2730.
- (14) Trevisan, C. S.; Orel, A. E.; Rescigno, T. N. Ab Initio Study of Low-Energy Electron Collisions with Ethylene. *Phys. Rev. A* **2003**, *68*, No. 062707.
- (15) Winstead, C.; McKoy, V.; Bettega, M. H. F. Elastic Electron Scattering by Ethylene, C_2H_4 . *Phys. Rev. A* **2005**, *72*, No. 042721.
- (16) Naghma, R.; Antony, B. Total Scattering Cross Sections for Ethylene by Electron Impact for Incident Electron Energies from 1 to 2000 eV. *Int. J. Quantum Chem.* **2014**, *114*, 271–277.
- (17) Kukulin, V. I.; Krasnopolsky, V. M. Description of Few-Body Systems via Analytical Continuation in Coupling Constant. *J. Phys. A* **1977**, *10*, L33–L37.
- (18) Krasnopolsky, V. M.; Kukulin, V. I. Theory of Resonance States Based on Analytical Continuation in the Coupling Constant. *Phys. Lett. A* **1978**, *69*, 251–254.
- (19) Horáček, J.; Mach, P.; Urban, J. Calculation of S-Matrix Poles by Means of Analytic Continuation in the Coupling Constant: Application to the $^2\Pi_g$ State of N_2^- . *Phys. Rev. A* **2010**, *82*, No. 032713.
- (20) Nestmann, B.; Peyerimhoff, S. D. Calculation of the Discrete Component of Resonance States in Negative Ions by Variation of Nuclear Charges. *J. Phys. B* **1985**, *18*, 615–626.
- (21) Nestmann, B.; Peyerimhoff, S. D. CI Method for Determining the Location and Width of Resonances in Electron–Molecule Collision Processes. *J. Phys. B* **1985**, *18*, 4309–4319.
- (22) Kukulin, V. I.; Krasnopolsky, V. M.; Horáček, J. *Theory of Resonances: Principles and Applications*; Kluwer Academic Publishers: Dordrecht, The Netherlands, 1988.
- (23) Tanaka, N.; Suzuki, Y.; Varga, K. Exploration of Resonances by Analytic Continuation in the Coupling Constant. *Phys. Rev. C* **1997**, *56*, 562–565.
- (24) Aoyama, S. Theoretical Prediction for the Ground State of ^{10}He with the Method of Analytic Continuation in the Coupling Constant. *Phys. Rev. Lett.* **2002**, *89*, No. 052501.
- (25) Funaki, Y.; Horiuchi, H.; Tohsaki, A. New Treatment of Resonances with a Bound State Approximation Using a Pseudo-Potential. *Prog. Theor. Phys.* **2006**, *115*, 115–127.
- (26) Si-Chun, Y.; Jie, M.; Shan-Gui, Z. Exploration of Unbound States by Analytical Continuation in the Coupling Constant Method within Relativistic Mean Field Theory. *Chin. Phys. Lett.* **2001**, *18*, 196–198.
- (27) Cattapan, G.; Maglione, E. From Bound States to Resonances: Analytic Continuation of the Wave Function. *Phys. Rev. C* **2000**, *61*, No. 067301.
- (28) Papp, P.; Matejčík, Š.; Mach, P.; Urban, J.; Paidarová, I.; Horáček, J. Analytical Continuation in Coupling Constant Method; Application to the Calculation of Resonance Energies and Widths for Organic Molecules: Glycine, Alanine and Valine and Dimer of Formic Acid. *Chem. Phys.* **2013**, *418*, 8–13.
- (29) Baker, G. A.; Graves-Morris, P. *Padé Approximants*; Addison-Wesley: Reading, MA, 1981.
- (30) Krasnopolsky, V. M.; Kukulin, V. I.; Horáček, J. Construction of S-matrix from Scattering Data. *Czech. J. Phys. B* **1985**, *35*, 805–819.
- (31) Krasnopolsky, V. M.; Kukulin, V. I.; Kuznetsova, E. V.; Horáček, J. Padé-Approximant Techniques for Processing Scattering Data. II. Energy-Dependent Phase-Shifts Analysis of Low-Energy $^4\text{He} + ^2\text{H}$ Scattering. *Czech. J. Phys. B* **1990**, *40*, 945–1064.
- (32) Horáček, J.; Zejda, L.; Queen, N. M. Comparative Study of Methods for the Construction of Padé Approximants of Type III. *Comput. Phys. Commun.* **1993**, *74*, 187–192.
- (33) Krasnopolsky, V. M.; Kukulin, V. I.; Kuznetsova, E. V.; Horáček, J.; Queen, N. M. Energy-Dependent Phase-Shift Analysis of $^2\text{H} + ^4\text{He}$ Scattering in the Energy Range $0.87 < E_d < 5.24$ MeV. *Phys. Rev. C* **1991**, *43*, 822–834.
- (34) Bessis, D. Padé Approximations in Noise Filtering. *J. Comput. Appl. Math.* **1996**, *66*, 85–88.
- (35) Knowles, P. J.; Hampel, C.; Werner, H.-J. Coupled Cluster Theory for High Spin, Open Shell Reference Wave Functions. *J. Chem. Phys.* **1993**, *99*, 5219–5227; Erratum: **2000**, *112*, 3106–3107.
- (36) Deegan, M. J. O.; Knowles, P. J. Perturbative Corrections To Account for Triple Excitations in Closed and Open Shell Coupled Cluster Theories. *Chem. Phys. Lett.* **1994**, *227*, 321–326.
- (37) Werner, H.-J.; Knowles, P. J.; Knizia, G.; Manby, F. R.; Schutz, M.; et al. *MOLPRO: A Package of Ab Initio Programs*, version 2010.1; <http://www.molpro.net>.
- (38) Dunning, T. H., Jr. Gaussian Basis Sets for Use in Correlated Molecular Calculations. I. The Atoms Boron through Neon and Hydrogen. *J. Chem. Phys.* **1989**, *90*, 1007–1023.